文章编号 1004-924X(2009)06-1385-06

采用环形岛棱结构的电容式压力传感器

邹黎明, 郭 航
(厦门大学 萨本栋微机电研究中心, 福建 厦门 361005)

摘要: 改变传感器可动极板的结构是解决 MEMS 电容式压力传感器信号输出与压力输入呈非线性关系问题的方法之一。设计了一种新型结构电容式压力传感器, 其可动极板是 LPCVD 氮化硅构成的一个方形薄膜, 薄膜中心到边缘之间由 PECVD 氧化硅构筑一个环形岛棱, 使可动极板在压力负载下的变形趋于平整, 减小了边缘杂散电容带来的非线性, 从而改善了该传感器的输出特性。利用有限元方法分析了不同尺寸的动极板在不同外加压力作用下压力与形变的关系, 以及相应的应力分布情况, 并采用最小二乘拟合直线法计算了压力传感器的线性度。分析结果表明, 与常规的双极板微型电容式压力传感器相比, 新型结构压力传感器的线性度改善了 48.38%, 达到了 1.6%。

关 键 词: 微机电系统; 电容式压力传感器; 线性度; 有限元法
中图分类号: TP212.12　　文献标识码: A

Capacitive pressure sensor with circular island structure

ZOU Li-ming, GUO Hang

(Pen-Tung Sah MEMS Research Center, Xiamen University, Xiamen 361005, *China)*

Abstract: A capacitive pressure sensor with a new movable electric plate structure is presented to improve the output nonlinearity of a MEMS-based capacitive pressure sensor. The movable plate of the sensor is a rectangular memrance made of LPCVD silicon nitride film, and a circular island is added from the center to the edge of the membrane by depositing and patterning a layer of PECVD silicon dioxide. With this structure, the deformation of the movable plate of the capacitive pressure sensor will tend to flat when applying a load of pressure, so that the nonlinearity of stray capacitance near the edge of the entire structure is decreased and the output properties of the sensor is improved. Moreover, the Finite Element Model(FEM) in ANSYS is used to analyze the new structure of the movable electrical plate with different dimensions to obtain the relationship between deflection and pressure and the corresponding stress distribution and a curve fitting based on the least-square method is applied to calculate the output linearity of the sensor. Comparison of the MEMS-based capacitive pressure sensor with a general structure sensor, the output linearity of the proposed sensor has been improved by 48.38%, reaching 1.6%.

Key words: MEMS; capacitive pressure sensor; linearity; Finite Element Method(FEM)

Received date: 2009-01-20; **Revised date:** 2009-04-30.

Foundation item: Supported by the National Plan for Undergraduate Experimental Creative Investigation (Grant No. 200810221871 2)

1 Introduction

The application of MEMS to the pressure measurement is a mature application of micro-machined silicon sensors, and devices have been around for more than 30 years. Pressure sensors have been developed by the use of a wide range of sensing techniques, from prevailing sensors of piezoresistive type to high-performance resonant pressure sensors[1]. Compared with other pressure sensors, the main attractions of capacitive pressure sensors are robust structure, high sensitivity, high stability, no turn-on temperature drift, and low temperature cross-sensitivity[2]. Generally, gap tuning, area tuning and dielectric tuning are three configurations for a simple parallel-plate capacitor structure.

For a traditional capacitive pressure sensor, it is based on a parallel-plate arrangement where one electrode is fixed and the other is flexible. As the flexible electrode deflects under applied pressure, the gap between electrodes decreases and the capacitance increases[3]. However, the main drawback associated with the capacitive pressure sensor is the inherently nonlinear output signal. In order to decrease the nonlinearity, one approach is to modify the shape of the electrical plate structure of the capacitor, such as using a tripled-layered composite membrane structure[4]; and the other is to design a well-matched circuitry interface or to use touch mode capacitive pressure sensor[2]. In this paper we present and investigate a new capacitive pressure sensor, which is based on a Si_3N_4/SiO_2 composite diaphragm structure.

2 Design for sensor structure and modeling

In order to ameliorate the linearity of the pressure sensor, we design a capacitive pressure sensor with a new film structure, which is shown in Fig. 1. And the Si_3N_4/SiO_2 composite diaphragm structure is shown in Fig. 2.

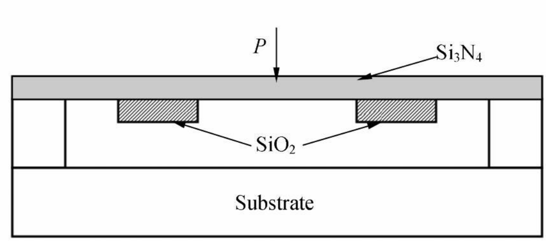

Fig. 1 Cross-section of a capacitive pressure sensor with composite diaphragm structure

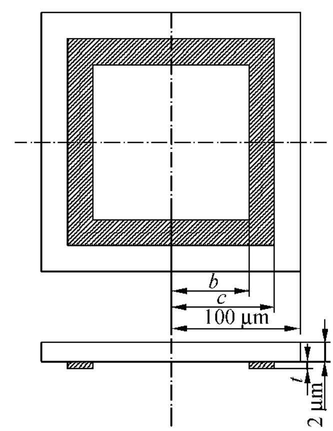

Fig. 2 Si_3N_4/SiO_2 composite-diaphragm structure

The new sensor structure consists of two materials. The first Si_3N_4 thin film is grown on the silicon´s substrate by using the low-pressure chemical vapor deposition (LPCVD) method. Then the wafer is covered by a plasma-enhanced chemical vapor deposition (PECVD) SiO_2. After that, we pattern the SiO_2 thin film and use wet etching to it, in order to obtain the different dimensions that we need.

The capacitance between two parallel electrodes of a traditional capacitive pressure sensor can be expressed as

$$C = \frac{\varepsilon_0 \varepsilon_r A}{d}, \quad (1)$$

where, ε_0, ε_r, A, and d are the permittivity of free space (8.854×10^{-12} F/m), relative dielectric constant of the material between the plates (which is unity for air), effective electrode are-as, and the gap between the plates. For a square diaphragm, which is bent under an external pressure applied to it, the corresponding change in capacitance is given by the following double-integral form which is

$$C = \iint \frac{\varepsilon_0 \varepsilon_r}{d - w(x, y)} \mathrm{d}x \mathrm{d}y , \qquad (2)$$

where $w(x, y)$ is the deflection of the square diaphragm. The deflection can be applied to pressure by[5]

$$P = \frac{Eh^4}{(1-\nu^2)a^4}\left[4.20\frac{w_0}{t} + 1.58\frac{w_0^3}{t^3}\right] , \qquad (3)$$

where a, t, ν and E are a half length of one side of the diaphragm, the thickness, poisson ratio and Young's modulus, respectively, and w_0 is the maximum deflection of the diaphragm. Eq. (3) provides a reasonable approximation of the maximum deflection over a wide range of pressure values, but it is not limited to small deflections. The first term within Eq. (3) dominates most for small deflections, for which $w_0 < t$, whereas the second term dominates most for large deflections. Based on the energy theory, the deflection function of the diaphragm is given by[6]

$$w(x, y) = w_0(1-X^2)^2(1-Y^2)(1+mX^2+ mY^2+nX^2Y^2) , \qquad (4)$$

where $X = x/a$, $Y = y/a$, and the coefficient of m is 0.264 and n is 0.309. In this paper, we only consider the small deflection of the diaphragm.

3 Analysis and optimization

3.1 Linearity analysis

As a comparison, a traditional sensor is studied. The material of the diaphragm is Si_3N_4, and the diaphragm is designed with a thickness of 2 μm and a length of 200 μm for one side. The gap between plates of the capacitive sensor is 3 μm. We use Eqs. (2)-(4) to calculate the relationship between pressure and capacitance, and it is shown in Fig. 3.

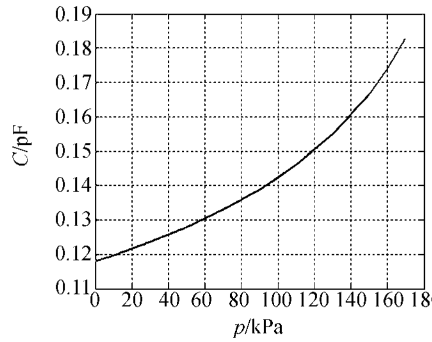

Fig. 3 Relationship between pressure and capacitance of a traditional capacitive pressure sensor

Linearity can be defined as the adjacence degree which denotes how a curve fits a straight line. Independent linearity, terminal-based linearity and zero-based linearity are three definitions used in the specification of pressure sensors. We use the least square method to fit the curve, and the linearity of the traditional capacitive pressure sensor is 3.1%.

We use ANSYS to analyze the relationship of pressure and capacitance for the new structure capacitive pressure sensor. As shown in Fig. 4, the Si_3N_4/SiO_2 composite diaphragm structure is

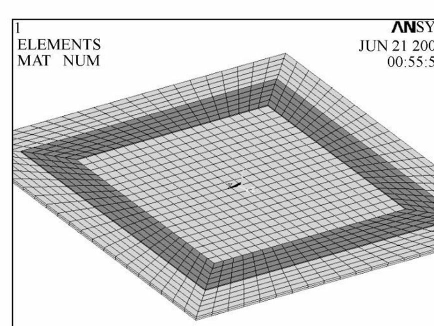

Fig. 4 Finite element model of a Si_3N_4/SiO_2 composite diaphragm structure in ANSYS

modeled by using the 3-D element, Solid 45, in ANSYS. Young's modulus and Poisson's ratio of the structure are shown in Tab. 1. For this new structure, the dimension of Si_3N_4 is the same as that in the traditional capacitive pressure sensor above. The thickness of the SiO_2 diaphragm is 0.5 μm, while b= 60 μm and c= 80 μm (b and c are shown in Fig. 2). The capacitance C of the capacitive pressure sensor can be calculated by

$$C=\varepsilon_0\varepsilon_{SiO_2}\varepsilon\iint_{A_{SiO_2}}\frac{1}{\varepsilon t_{SiO_2}+\varepsilon_{SiO_2}(d-t_{SiO_2}-w(x,y))}\mathrm{d}\sigma+$$
$$\varepsilon_0\varepsilon_r\iint_{A-A_{SiO_2}}\frac{1}{d-w(x,y)}\mathrm{d}\sigma. \quad (5)$$

Tab. 1 Mechanical properties of materials for finite element analysis

	Young's modulus (GPa)	Poisson ratio
silicon nitride	200	0.27
silicon dioxide	0.73	0.17

The deflection of the Si_3N_4/SiO_2 composite diaphragm under the pressure of 50 kPa is given in Fig. 5, and the maximum deflection w_0 in the

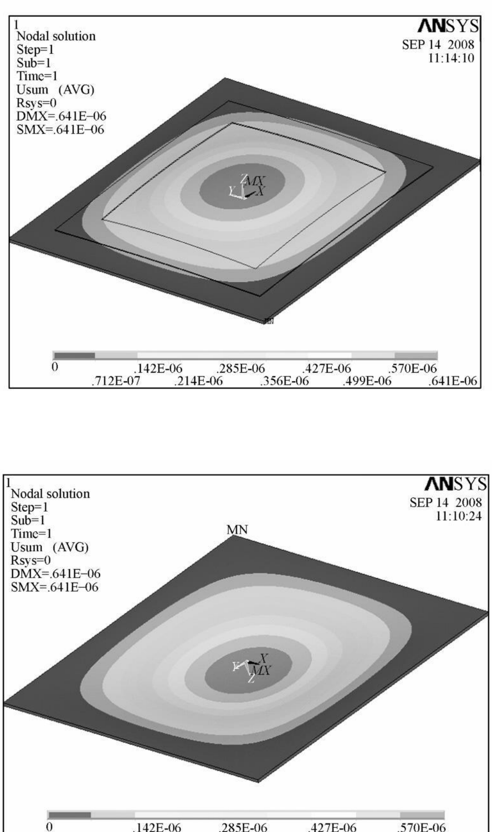

Fig. 5 Contours of deflection of composite diaphragm structure under a pressure of 50 kPa

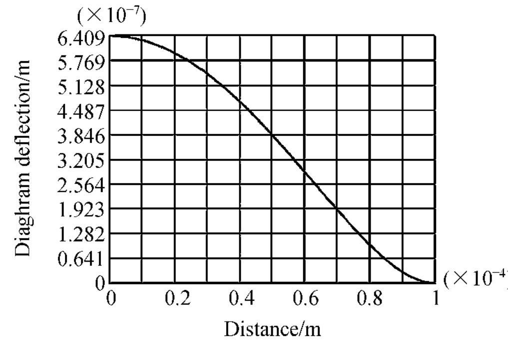

(a) ANSYS analysis

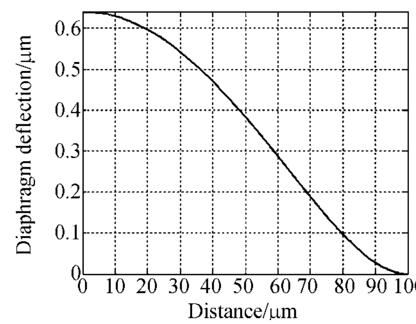

(b) Modeling analysis

Fig. 6 Comparison of curves of bent diaphragm between ANSYS and modeling

center of diaphragm is obtained. The shape curves of the bent diaphragm are described in Fig. 6 (a) and Fig. 6 (b), which is obtained from the FEM (finite element model) and Eq. (4), respectively. Comparing Fig. 6 (a) with Fig. 6(b), we can see that a good agreement between them has been achieved. The maximum stress of the Si_3N_4 diaphragm is 0.121 GPa, which occurs along the edges of the diaphragm, while the maximum one is 0.028 GPa in the SiO_2 diaphragm. Both of them are smaller than their yield strengths. The stress distribution of the diaphragm is shown in Fig. 7. The linearity of a capacitive pressure sensor with that of a new film structure is 2.1%, which is declined by 31.5% compared with a traditional capacitive pressure sensor.

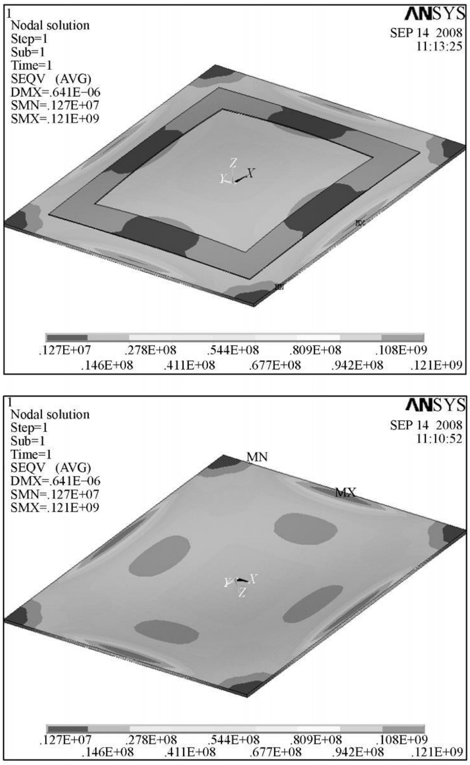

Fig. 7 Contours of stress distribution of composite diaphragm structure

3.2 Optimization of device

Through the analysis above, it is a good approach to improve the linearity of the capacitive pressure sensor apparently. Furthermore, we optimize the dimensions of the SiO_2 diaphragm in order to obtain a better linearity. First, we assume that $b = 60$ μm, $c = 80$ μm with the SiO_2 diaphragm, the linearity of the novel capacitive pressure sensor are 2.8% and 2.1% when the thickness of SiO_2 is 0.3 μm and 0.5 μm, respectively. The relationship between pressure and capacitance is shown in Fig. 8, and it can be seen thatthe thicker SiO_2 diaphragm has a better linearity. When the thickness of SiO_2 diaphragm is fixed at 0.5 μm and the length of one side of SiO_2 diaphragm varies, the relationship between pressure and capacitance is shown in Fig. 9. The

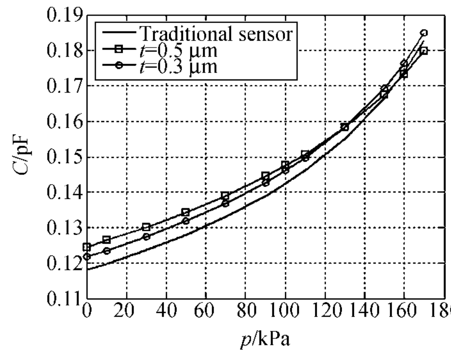

Fig. 8 Relationship between pressure and capacitance ($b = 60$ μm, $c = 80$ μm)

best result for the linearity is 1.6%, as shown in Tab. 2. Thus, the linearity is further improved from 2.1% to 1.6%.

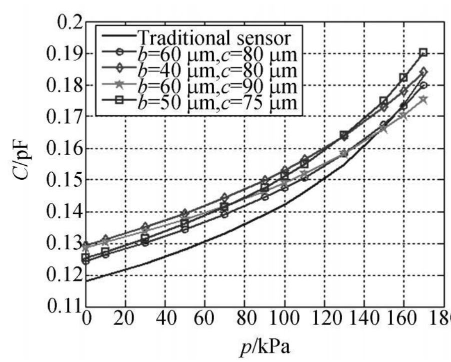

Fig. 9 Relationship between pressure and capacitance with differents dimensions of the SiO_2 diaphragm ($t_{SiO_2} = 0.5$ μm)

Tab. 2 Linearity values with different dimensions of SiO_2 diaphragm

Dimension	Linearity value(%)
The traditional sensor	3.1
$b = 60$ μm, $c = 80$ μm	2.1
$b = 40$ μm, $c = 80$ μm	1.9
$b = 60$ μm, $c = 90$ μm	1.6
$b = 50$ μm, $c = 75$ μm	2.6

4 Conclusions

In this paper, a new capacitive pressure sensor with Si_3N_4/SiO_2 composite diaphragm structure is presented. Through the analysis and optimization, the linearity values of pressure sensor with the new structure can be effectively improved and the optimized result is 1.6%.

References:

[1] BEEBY S, ENSELL G, KRAFT M, *et al*.. *MEMS Mechanical Sensors* [M]. London: Artech House, 2004.

[2] KO W H, WANG Q. Touch mode capacitive pressure sensors [J]. *Sensors and Actuators*, 1999, 75(3): 242-251.

[3] VARADAN V K, VINOY K J, JOSE K A. *RF MEMS and Their Applications* [M]. USA: John Wiley, 2003.

[4] ZHOU M X, HUANG Q A, QIN M. Modeling, design and fabrication of a triple-layered capacitive pressure sensor [J]. *Sensors and Actuators*, 2005, 117(1): 71-81.

[5] GAG-EL-HAK M. *MEMS: Applications* [M]. 2nd ed. New York: Taylor and Francis, 2006.

[6] TIMOSHENKO S P, KRIEGER S W. *Theory of Plates and Shells* [M]. 2nd ed. New York: McGraw-Hill, 1940.

Authors' biographies:

ZOU Li-ming (1983-), male, conducts research at the Pen-Tung Sah MEMS Research Center, Xiamen University. His research focus on micro-sensors, microstructure fabrication and piezoelectric devices. **E-mail:** mingzhixue@163.com

GUO Hang (1967-), male, professor of the Pen-Tung Sah MEMS Research Center, Xiamen University, his research interests include the design and fabrication of integrated circuits, micro electromechanical system and nano technology. **E-mail:** hangguo@xmu.edu.cn

●下期预告

天文导航中星敏感器关键技术现状及发展

李葆华, 刘国良, 刘　睿, 王常虹

(哈尔滨工业大学 空间控制与惯性技术研究中心, 黑龙江 哈尔滨 150001)

星敏感器仅仅工作在全天球的识别模式下远远不能满足当前飞行器任务的需要。当星敏感器有足够的先验信息时, 可在星跟踪模式或者预测星像模式下工作。这些算法不但提高了星敏感器的数据更新率, 而且降低了由于全天球识别带来误匹配的可能性。为了克服由于飞行器大角速度情况下传统星跟踪算法的时间长等不足, 文中提出了一种新的星跟踪算法; 为了消除由于系统噪声带来的误差, 提出了星图滤波和星像滤波的方法。实验结果表明, 当飞行器在 2.25°/s 的角速度下, 星敏感器能在 10×10 的范围内从星图中正确提取星像, 星图经去噪后, 星敏感器输出精度提高了近 5″。从而使飞行器可在高动态情况下, 星敏感器输出高精度、高更新率的姿态。文中描述的所有方法已经在 2007 年和 2008 年进行了地面观星测试, 并于 2009 年即将应用于某些卫星的姿控系统中。部分算法已在 2005 年搭载于某卫星进行了在轨试验。